Supporting Information

Glycoside Hydrolase Catalysis: Do Substrates and Mechanism-Based Covalent Inhibitors React via Matching Transition States?

Oluwafemi Akintola,[1] Marco Farren-Dai,[1] Weiwu Ren,[1] Sandeep Bhosale,[1] Robert Britton,[1] Katarzyna Świderek,[2] Vicent Moliner,[2,*] and Andrew J. Bennet[1,*]

[1] Department of Chemistry, Simon Fraser University, Burnaby, British Columbia, Canada, V5A 1S6
[2] BioComp Group, Institute of Advanced Materials (INAM), Universitat Jaume I, 12071 Castellón, Spain.

Corresponding authors Andrew J. Bennet, e-mail bennet@sfu.ca; Vicent Moliner, e-mail moliner@uji.es.

Table of contents

Materials and General procedures

All reactions described, except otherwise specified, were performed under an atmosphere of dry nitrogen using flame/oven-dried glassware. Thin-layer chromatography (TLC) plates used were made from aluminum plates pre-coated with silica gel 60F-254 as the adsorbent. To aid visualization, the developed TLC plates were exposed to UV light and/or sprayed with a solution containing 1% $Ce(SO_4)_2$ and 1.5% molybdic acid in 10% aqueous H_2SO_4 and heated. Concentration and removal of trace solvents was done with a Büchi rotary evaporator using a dry ice/acetone condenser and vacuum applied from a Büchi V-500 pump. Automated flash chromatography on an automated system using pre-packed high-performance RediSep Rf Gold flash columns packed with 20−40 μM spherical silica gel. All reagents, solvents, and starting materials were purchased from Carbosynth, Sigma-Aldrich, TCI America, Caledon, Fisher, Strem, Alfa Aesar, EMD, Anachemia, or ACP and were used without further purification unless otherwise specified. Tetrahydrofuran (THF) was freshly distilled over Na metal/benzophenone. ^{1}H and ^{13}C NMR spectra were recorded on either a Bruker 400 (400 MHz) instrument using $CDCl_3$ and CD_3OD as solvents. Chemical shifts are reported in ppm downfield to tetramethylsilane (δ 0) and were measured relative to the signal of the solvent (^{1}H NMR: $CDCl_3$: δ 7.26, CD_3OD: δ 3.31; ^{13}C NMR: $CDCl_3$: δ 77.16, CD_3OD: δ 49.00). Coupling constants (*J* values) are given in Hertz (Hz) and are reported to the nearest 0.1 Hz. ^{1}H NMR spectral data are tabulated in the order: multiplicity (s, singlet; d, doublet; t, triplet; q, quartet; m, multiplet; br., broad), coupling constants, number of protons were applicable. All NMR peaks were assigned using ^{1}H–^{1}H COSY and ^{1}H–^{13}C HSQC 2D spectra. High-resolution mass spectra were acquired on a Bruker maXis Impact TOF LC/MS/MS system. The synthesis and characterization of compounds **3**, **4**, **5**, **6**, and **7** were previously published.[1]

Synthesis of 6-fluoro-4-methylumbelliferyl β-D-melibioside

2,3,4,6-Tetra-*O*-acetyl-α-D-galactopyranosyl-(1→6)-2,3,4-tri-*O*-acetyl-α,β-D-glucopyranose (S3). D-Melibiose monohydrate (**S1**, α-D-galactopyranosyl-(1→6)-D-glucopyranose; 10 g, 27.8 mmol) was dissolved in anhydrous pyridine (36 mL) and Ac_2O (42 mL, 440 mmol) was added. After 72 h, dichloromethane (500 mL) was added, and the solution was washed with 2 M HCl (2 × 200 mL). The absence of pyridine was confirmed by TLC under UV light. The extract was then washed with $NaHCO_3$ (200 mL), dried over Na_2SO_4, and then concentrated *in vacuo* to yield peracetylated melibiose **S2** as a viscous oil in a quantitative yield. Melibiose octa-acetate **S2** (5 g, 7.4 mmol) was then dissolved in anhydrous dimethylformamide (30 mL) and ammonium acetate (1.15 g, 0.15 mmol) was added. After

72 h, the reaction mixture contained no remaining starting material (TLC analysis), and dichloromethane (100 mL) was added. This solution was washed with water (3 × 300 mL), brine, dried (Na_2SO_4), filtered, and the filtrate was then concentrated *in vacuo* to yield a viscous oil. Purification by flash chromatography on silica gel (3-5% MeOH in CH_2Cl_2) gave the hemiacetal **S3** (3.2 g, 68%) as a faintly yellow viscous oil, which was a mixture of α:β anomers in ratio ~ 7:3. (3.2 g, 68%) as a viscous oil. ^{1}H NMR (400 MHz, $CDCl_3$) δ 5.55 (dd, *J* = 10.2, 9.4 Hz, 1H), 5.43 (dd, *J* = 10.1, 3.5 Hz, 2.4H), 5.38–5.29 (m, 1.4H), 5.24 (t, *J* = 9.5 Hz, 0.4H), 5.16 (d, *J* = 3.7 Hz, 1.4H), 5.12–5.03 (m, 1.3H), 4.95 (dt, *J* = 15.7, 9.6 Hz, 1.4H), 4.89–4.82 (m, 1.3H), 4.76 (d, *J* = 8.0 Hz, 0.4H), 4.37 (t, *J* = 6.9 Hz, 0.4H), 4.32–4.11 (m, 3.1H), 4.01 (dd, *J* = 11.2, 7.3 Hz, 1.3H), 3.81–3.63 (m, 4.1H), 2.14 (s, 4.3H), 2.10 (m, 7.4H), 2.06–2.04 (m, 8.6H), 2.01 (s, 4.3H), 1.99 (s, 4.4H).

6-Fluoro-4-methylumbelliferyl 2,3,4,6-tetra-*O*-acetyl-α-D-galactopyranosyl-(1→6)-2,3,4-tri-*O*-acetyl-β-D-glucopyranoside (S4). To a cooled (0 °C) solution of anhydrous THF (20 mL), triphenylphosphine (1.54 g, 5.88 mmol) and DIAD (1.2 mL, 5.88 mmol) were added and stirred vigorously to this mixture protected melibiose hemiacetal **S3** (1.25 g, 1.96 mmol) was added, followed 10 min later by the addition of 6-fluoro-4-methylumbelliferone (0.38 g, 1.96 mmol). The resulting mixture was stirred for 1 h at 0 °C and was monitored by TLC analysis and when the starting material had been consumed, water (100 mL) was added. The reaction mixture was dissolved in water (100 mL) and extracted with ethyl acetate (3 × 100 mL). The combined organic layers were washed with brine, dried (Na_2SO_4), and concentrated *in vacuo*. The resulting crude residue was purified by flash chromatography (45−55% ethyl acetate in hexanes) to afford the protected 6-fluoro-4-methylumbelliferone melibioside **S4** (α:β ratio 1:4) as a colorless solid (620 mg, 42%). ^{1}H NMR (400 MHz, $CDCl_3$) δ 7.38 (d, *J* = 10.7 Hz, 0.3H), δ 7.35 (d, *J* = 10.7 Hz, 1H), 7.16 (d, *J* = 6.8 Hz, 0H), 7.10 (d, *J* = 6.9 Hz, 1H), 6.26–6.20 (m, 1.3H), 5.74–5.67 (m, 0.6H), 5.38 (dd, *J* = 3.4, 1.3 Hz, 0.3H), 5.36–5.25 (m, 4.3H), 5.25–5.17 (m, 1.3H), 5.16–5.08 (m, 5H), 5.00 (dd, *J* = 10.3, 3.7 Hz, 0.3H), 4.32 (ddd, *J* = 10.4, 6.3, 2.1 Hz, 0.3H), 4.20–4.10 (m, 1.3H), 4.09–3.98 (m, 2.5H), 3.87 (ddd, *J* = 9.9, 6.4, 2.3 Hz, 1H), 3.77 (m, 1.3H), 3.57 (dd, *J* = 11.2, 2.4 Hz, 1H), 3.52 (dd, *J* = 11.1, 2.2 Hz, 0.3H), 2.39 (m, 3.7H), 2.15 (s, 3H), 2.13–2.10 (m, 5.3H), 2.08 (d, *J* = 1.8 Hz, 6.6H), 2.06 (s, 0.8H), 2.04 (m, 6.7H), 1.94 (m, 2.8H). HRMS *m/z*: $(M + Na)^+$ calcd for $C_{36}H_{41}FO_{20}Na$, 835.2067; found 835.2062.

6-Fluoro-4-methylumberiferyl α-D-galactopyranosyl-(1→6)-β-D-glucopyranoside (1) The protected 6-fluoro-4-methylumbelliferone melibioside **S4** (430 mg, 0.53 mmol) was dissolved in methanol (4 mL) and a catalytic amount of potassium carbonate (7.3 mg, 0.053 mmol) was added. The reaction mixture

was stirred for 16 h at rt, concentrated *in vacuo,* and the resulting pale yellow oil was purified by flash chromatography (15% methanol in dichloromethane) to give pure β-anomer **1** (150 mg, 55%) and a mixture of the two anomers (57 mg, 21%) as colorless solids. Compound **1**, mpt = 113–114 °C; ^{1}H NMR (400 MHz, CD_3OD): δ 7.57 (d, *J* = 11.2 Hz, 1H, Ar-H), 7.43 (d, *J* = 7.0 Hz, 1H, Ar-H), 6.30 (d, *J* = 1.4 Hz, 1H, Ar-H), 5.09 (d, *J* = 7.3 Hz, 1H, H-1'), 4.88 (d, *J* = 3.8 Hz, 1H, H-1), 4.08 (dd, *J* = 10.1, 3.3 Hz, 1H, H-3), 3.90 (dd, *J* = 9.9, 7.1 Hz, 1H, H-6a), 3.86–3.75 (m, 4H, H-2, H-5, H-5', H-6b), 3.70 (dd, *J* = 3.4, 1.2 Hz, 1H, H-4), 3.65–3.47 (m, 4H, H-2', H-3', H-6a', H-6b'), 3.36 (m, 1H, H-5), 2.44 (d, *J* = 1.2 Hz, 3H, $–CH_3$); ^{13}C NMR (101 MHz, CD_3OD) δ 163.44 (C=O), 155.34 (d, *J* = 2.7 Hz, Ar-C), 151.43 (d, *J* = 1.9 Hz, Ar-C), 150.76 (d, $^{1}J_{C,F}$ = 245.5 Hz, Ar-C), 149.85 (d, *J* = 12.7 Hz, Ar-C), 115.70 (d, *J* = 7.5 Hz, −*C*=CH), 113.83 (−C=*C*H), 112.44 (d, *J* = 21.8 Hz, Ar-C), 106.85 (Ar−C), 102.37 (C-1'), 100.50 (C-1), 78.10 (C-3'), 77.14 (C-2), 74.82 (C-2'), 72.25 (C-5), 71.53 (C-4'), 71.28 (C-4), 71.24 (C-3), 69.94 (C-5'), 68.17 (C-6), 62.59 (C-6'), 18.73 ($-CH_3$); HRMS *m/z*: $(M + Na)^+$ calcd for $C_{22}H_{27}FO_{13}Na$, 541.1328; found 541.1319.

Scheme S1. Synthesis of 6-fluoro-4-methylumbelliferyl β-D-melibioside substrate (**1**) from melibiose (**S1**).

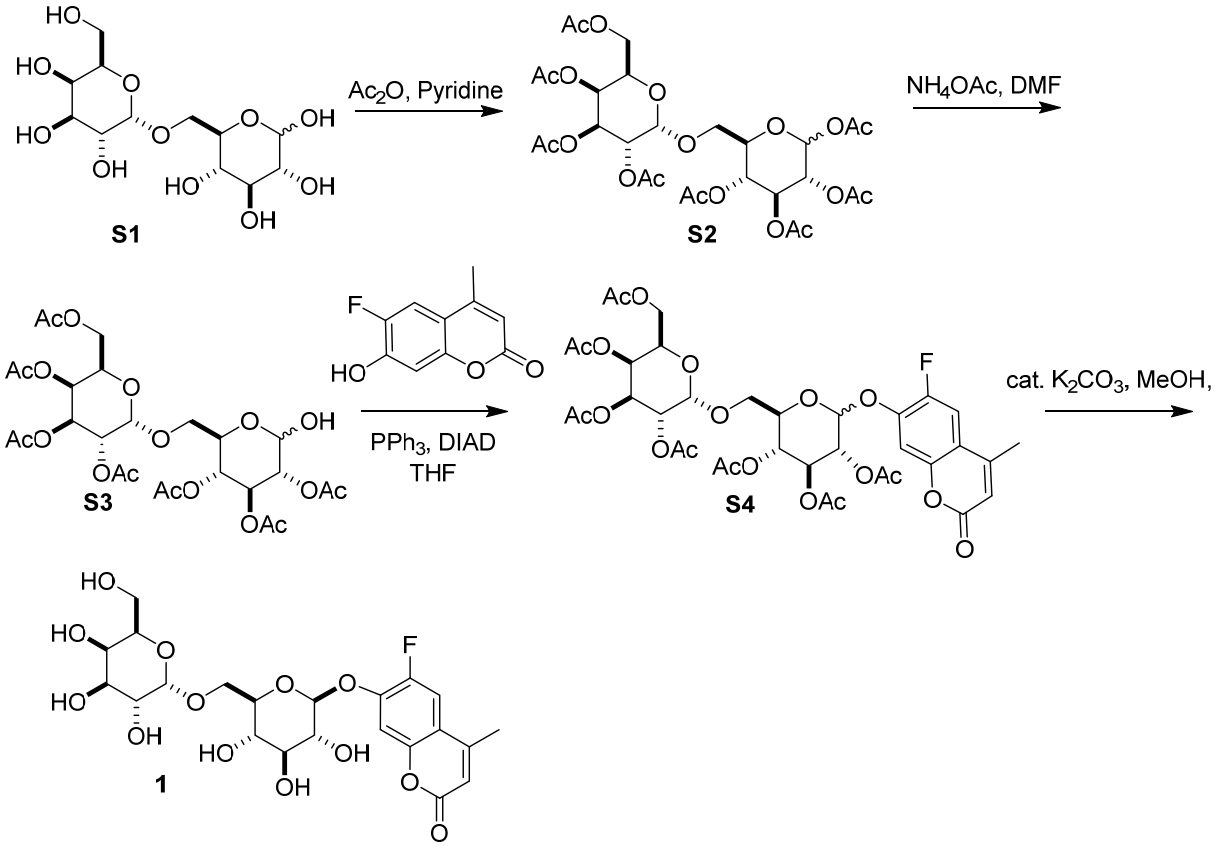

Scheme S2. Assay for α-galactosidase activity using 6-fluoro-4-methylumbelliferyl β-D-melibioside as substrate.

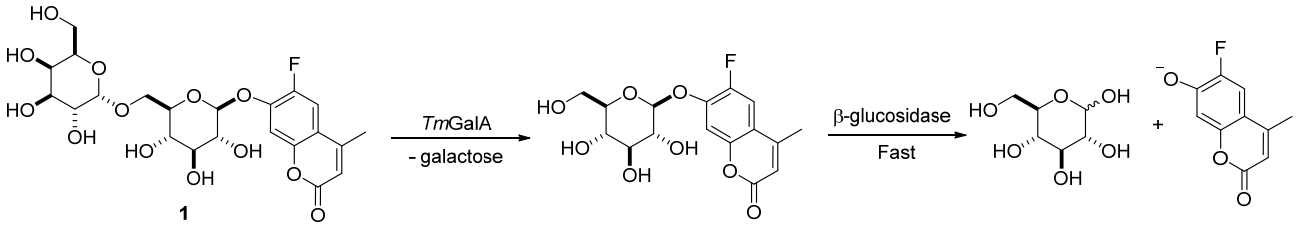

Scheme S3. Key distances used during the exploration of potential and free energy surfaces for the alkylation step of glycoside **3** (left) and carbasugar **4** (right).

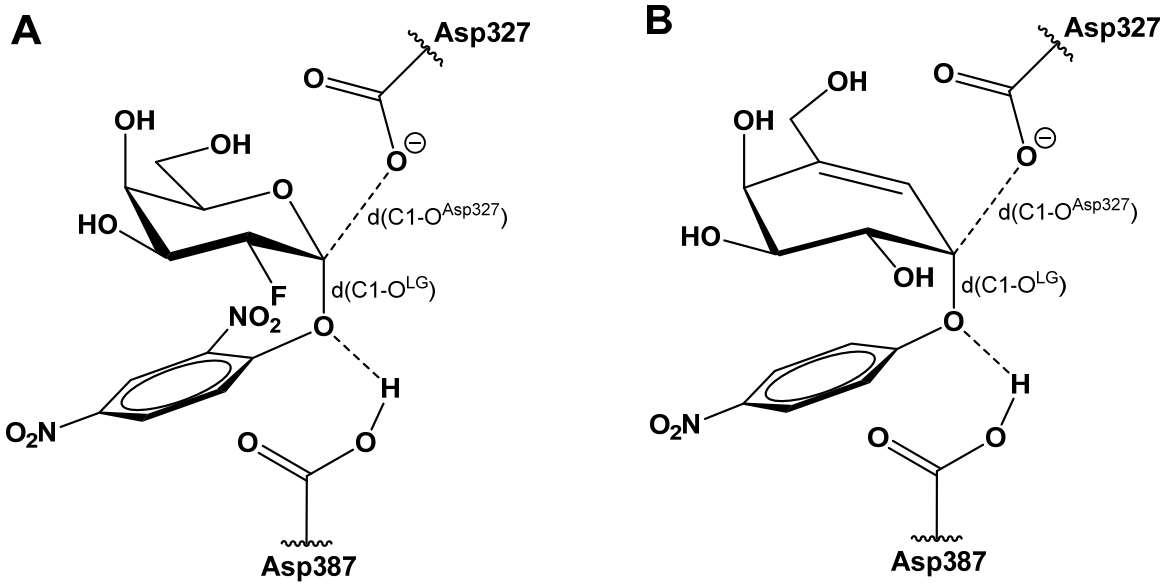

Table S1: Kinetic parameters for the pH-dependent hydrolysis of substrates **1** and **2** by *Tm*GalA WT. All experiments were performed at T = 37 °C, 50 mM buffer (MES buffer for pH 6.5, HEPES buffer for pH 7.0–7.5, glycylglycine buffer for pH 8.0–8.5, glycine-NaOH buffer for pH 9.0–10.0), and 0.1% BSA.

	6F4MU β-melibiose **1**		4NP α-galactoside **2**	
pH	K_m **(μM)**	k_{cat}/K_m **(mM^{-1} s^{-1})**	K_m **(μM)**	k_{cat}/K_m **(mM^{-1} s^{-1})**
6.5	10.5 ± 0.6	18.3 ± 1.4	66.6 ± 7.0	27.3 ± 3.4
7.0	6.7 ± 0.4	24.0 ± 1.6	14.4 ± 0.7	43.6 ± 2.7
7.5	6.0 ± 0.3	24.0 ± 1.6	14.5 ± 1.6	33.4 ± 4.5
8.0	12.3 ± 0.8	13.0 ± 1.1	30.7 ± 2.2	37.9 ± 3.2
8.5	14.8 ± 0.8	9.9 ± 0.6	30.9 ± 1.5	25.6 ± 1.6
9.0	22.1 ± 1.2	6.7 ± 0.5	26.2 ± 1.6	26.0 ± 1.9
9.5	25.5 ± 2.1	5.5 ± 0.6	30.5 ± 1.1	18.0 ± 0.8
10.0	28.7 ± 1.5	5.1 ± 0.4	41.2 ± 1.4	14.0 ± 0.6

Table S2: Forward primers used to generate mutant plasmids used to produce active-site variants of *T. maritima* α-galactosidase.

Variant	Primer (5" to 3")
D220S	TTCGAGGTCTTCCAGATAAGCGACGCCTACGAAAA
D220A	TTCGAGGTCTTCCAGATAGCCGACGCCTACGAAAA
D221S	TTCGAGGTCTTCCAGATAGACAGCGCCTACGAAAA
D221A	TTCGAGGTCTTCCAGATAGACGCCGCCTACGAAAA
W190F	CTGGATGGTGCAGCTTCTACCATTACTTCCT
Y191F	CTGGATGGTGCAGCTGGTTCCATTACTTCCT
D427S	CTGAACGACCCCAGCTGTCTGATACTG
W65F	CTGGCAGTCCTTTGGACCGTGCAGGGT
W65Y	CTGGCAGTCCTATGGACCGTGCAGGGT
C368A	CATCCTCGGAGCCGGCTCTCCCCTTC
C368S	CATCCTCGGATCCGGCTCTCCCCTTC
K325A	GGGCTACAGGTACTTCGCGATCGACTTTCTCTTCGCGGG
W257Y	CCCGGGCATATATACCGCCCCGTTCAG
W257F	CCCGGGCATATTTACCGCCCCGTTCAG

Table S3: Melting Temperatures (**T_m**) obtained from the thermal denaturation of *Tm*GalA WT and mutants by differential scanning fluorimetry.

Enzyme	Melting Temperature (T_m)	Hydrolysis of **2** [a,b]
WT	89.5 ± 0.3	Y
D220S	85.1 ± 0.0	< 0.10% [c]
D220A	83.0 ± 0.0	N.D.
D221S	87.7 ± 0.1	Y
D221A	86.8 ± 0.9	Y
W190F	84.7 ± 0.0	Y
Y191F	68.4 ± 1.2	~10%
D427S	89.2 ± 0.1	~0.2% [c]
W65F	90.0 ± 0.2	Y
W65Y	89.7 ± 0.1	Y
C368A	89.8 ± 0.0	Y
C368S	91.2 ± 0.3	Y
K325A	65.8 ± 0.2	N.D.
W257Y	68.7 ± 0.6	N.D.
W257F	91.5 ± 0.1	Y

[a] Conditions HEPES buffer (50 mM, pH = 7.4, 0.1% BSA), 37 °C and [**2**] = 0.25 mM. [b] Y = hydrolysis observed, N.D. = not detectable. [c] Relative to wild type *Tm*GalA.

Table S4: Kinetic parameters for the hydrolysis by TmGalA WT and mutant enzymes for substrates **1**, **2**, and **3**. All experiments were carried out at T = 37 °C in 50 mM glycylglycine buffer, pH 8.0 and 0.1 % BSA.

	6F4MU β-melibiose **1**		4NP α-galactoside **2**		DNP 2F-α-galactoside **3**	
Enzyme	K_m **(μM)**	k_{cat}/K_m **(mM^{-1} s^{-1})**	K_m **(μM)**	k_{cat}/K_m **(mM^{-1} s^{-1})**	K_m **(μM)**	k_{cat}/K_m **(mM^{-1} s^{-1})**
WT	12.0 ± 0.4	15.6 ± 0.6	30.7 ± 2.2	39.5 ± 3.5	318 ± 10.7	9.43 ± 0.43
D221S	32.8 ± 1.7	1.49 ± 0.10	731 ± 28	2.08 ± 0.12	4480 ± 120	0.22 ± 0.01
D221A	39.5 ± 2.3	0.20 ± 0.02	1100 ± 89	0.34 ± 0.04	3500 ± 120	0.12 ± 0.01
W65F	123.3 ± 5.0	1.46 ± 0.08	166 ± 9.2	14.05 ± 1.0	1130 ± 38	1.32 ± 0.06
W65Y	27.6 ± 1.2	2.61 ± 0.15	890 ± 36	7.29 ± 0.43	942 ± 75	1.70 ± 0.19
W190F	5.2 ± 0.7	3.68 ± 0.55	471 ± 12	5.22 ± 0.18	1280 ± 45	1.16 ± 0.06
Y191F	61.1 ± 2.1	0.11 ± 0.01	1970 ± 63	0.23 ± 0.01	1190 ± 39	0.08 ± 0.004
C368A	79.3 ± 1.7	2.84 ± 0.08	1070 ± 108	1.71 ± 0.26	1220 ± 62	0.26 ± 0.02
C368S	3.8 ± 0.1	24.8 ± 0.9	85.3 ± 4.7	23.3 ± 1.6	116 ± 6.0	2.59 ± 0.19
W257F	79.3 ± 2.6	2.59 ± 0.11	74.1 ± 4.2	10.8 ± 0.8	444 ± 13	0.70 ± 0.03

Table S5: Kinetic parameters for the covalent inhibition of *Tm*GalA WT and variants by various carbasugars. All experiments were carried out at T = 37 °C in 50 mM glycylglycine buffer, pH 8.0 and 0.1% BSA.

	Carbagalactose 4		**Carbagalactose 5**		**Carbasugar 6**	
***Tm*GalA**	K_m (μM)	k_{cat}/K_m (M^{-1} s^{-1})	K_m (μM)	k_{cat}/K_m (M^{-1} s^{-1})	K_m (μM)	k_{cat}/K_m (M^{-1} s^{-1})
WT	6.25 ± 0.43	81.3 ± 7.1	2.17 ± 0.16	(79.2 ± 8.0) × 10^3	51.6 ± 3.9	1660 ± 170
D221S		0.38 ± 0.009	18.7 ± 1.3	764 ± 75	1550 ± 95	4.52 ± 0.46
D221A		0.32 ± 0.005	54.0 ± 5.2	162 ± 23	2600 ± 110	1.03 ± 0.07
W65F	396 ± 65	1.39 ± 0.36	2.45 ± 0.21	3660 ± 420	30.1 ± 1.2	237 ± 14
W65Y	48.8 ± 9.8	3.29 ± 0.86	0.40 ± 0.05	(11.3 ± 1.6) × 10^3	63.7 ± 3.7	66.5 ± 5.0
W190F	478 ± 61	1.13 ± 0.23	16.5 ± 1.0	1590 ± 140	895 ± 21	9.3 ± 0.35
Y191F	1040 ± 130	0.32 ± 0.06	35.7 ± 2.3	409 ± 36	819 ± 100	1.02 ± 0.19
C368A	158 ± 23	2.25 ± 0.52	5.95 ± 0.44	365 ± 35	333 ± 26	5.78 ± 0.64
C368S	77.2 ± 2.8	10.7 ± 0.58	5.02 ± 0.53	8580 ± 1100	253 ± 15	107 ± 9.1
W257F	10.9 ± 1.1	6.69 ± 0.84	4.61 ± 0.43	1320 ± 183	118 ± 8.7	31.1 ± 3.14

Table S6: Kinetic parameters for the pH-dependent inhibition of *Tm*GalA WT by α-*galacto*-cyclophellitol **7**. All experiments were performed at T = 37 °C, 50 mM buffer (MES buffer for pH 6.5, glycylglycine buffer for pH 8.0–8.5, glycine-NaOH buffer for pH 10.0), and 0.1% BSA.

	α-*galacto*-cyclophellitol **7**	
pH	K_i **(μM)**	k_{inact}/K_i **(M^{-1} s^{-1})**
6.5	492 ± 52	8.1 ± 1.2
7.4	160 ± 21	1.0 ± 0.17
8.0	634 ± 52	1.3 ± 0.2
8.5	4990 ± 512	0.3 ± 0.04
10.0	14240 ± 1610	0.2 ± 0.01

Table S7: Kinetic parameters for the covalent inhibition of *Tm*GalA WT and variants by α-*galacto*-cyclophellitol **7**. All experiments were carried out at T = 37 °C in 50 mM glycylglycine buffer, pH 8.0 and 0.1% BSA.

Enzyme	K_i **(μM)**	k_{inact}/K_i **(M^{-1} s^{-1})**
WT	634 ± 52	1.32 ± 0.15
D221S	2620 ± 160	0.35 ± 0.03
D221A	3490 ± 260	0.11 ± 0.01
W65F	20.4 ± 3.3	68.0 ± 16.1
W65Y		0.34 ± 0.01
W190F	2080 ± 92	0.67 ± 0.04
Y191F	$(11.4 \pm 1.7) \times 10^3$	0.072 ± 0.017
C368A		0.52 ± 0.007
C368S	388 ± 43	1.85 ± 0.27
W257F		0.23 ± 0.004

TABLE S8: Missing atom types, charges and parameters for substrate **3**.

Atom Name	Atom Type	Charge (e^-)	Missing parameters
C1	c3	0.3199	IMPROPER
C2	c3	0.1006	ca-ca-ca-os 1.1 180.0 2.0
C3	c3	0.0821	ca-ca-ca-ha 1.1 180.0 2.0
C4	c3	0.1271	ca-ca-ca-no 1.1 180.0 2.0
C5	c3	0.1001	
C6	c3	0.1444	
C7	ca	0.2341	
C8	ca	-0.2050	
C9	ca	-0.0050	
C10	ca	-0.2132	
C11	ca	0.0100	
C12	ca	-0.2122	
F2	f	-0.2393	
N1	no	0.3212	
N2	no	0.3302	
O1	os	-0.3499	
O3	oh	-0.5978	
O4	oh	-0.5908	
O5	os	-0.3926	
O6	oh	-0.5988	
O7	o	-0.1950	
O8	o	-0.1950	
O9	o	-0.1955	
O10	o	-0.1955	
H1	h2	0.1027	
H2	h1	0.1027	
H3	h1	0.0737	
H4	h1	0.0717	
H5	h1	0.0957	
H6	h1	0.0697	
H7	h1	0.0697	
H8	ha	0.1740	
H9	ha	0.1850	
H10	ha	0.2080	
H12	ho	0.4220	
H13	ho	0.4240	
H14	ho	0.4170	

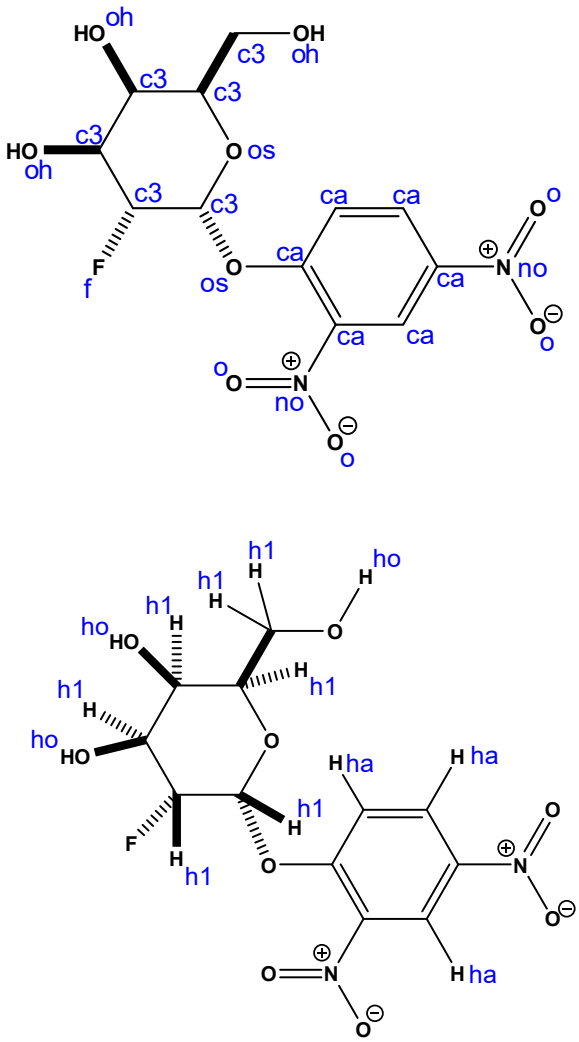

Table S9: Missing atom types, charges and parameters for inhibitor **4**.

Atom Name	Atom Type	Charge (e^-)	Missing parameters
C1	c3	0.1385	IMPROPER
C2	c3	0.1151	c2-c3-c2-c3 1.1 180.0 2.0
C3	c3	0.1231	c2-c3-c2-ha 1.1 180.0 2.0
C4	c3	0.1413	ca-ca-ca-os 1.1 180.0 2.0
C5	c2	-0.1422	ca-ca-ca-ha 1.1 180.0 2.0
C6	c3	0.1676	ca-ca-ca-no 1.1 180.0 2.0
C5a	c2	-0.1502	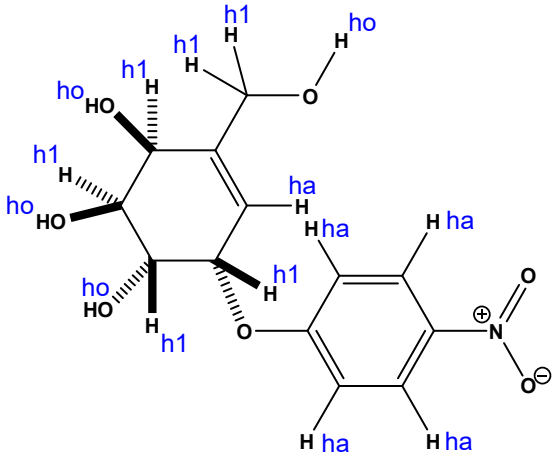
CO1	ca	0.1803	
CR1	ca	-0.1955	
CM1	ca	-0.0303	
CP	ca	-0.2182	
CM2	ca	-0.0303	
CR2	ca	-0.1955	
O1	os	-0.3279	
O2	oh	-0.5738	
O3	oh	-0.5778	
O4	oh	-0.6008	
O6	oh	-0.5968	
O1N	o	-0.2130	
O2N	o	-0.2130	
NO2	no	0.3192	
HC1	h1	0.0787	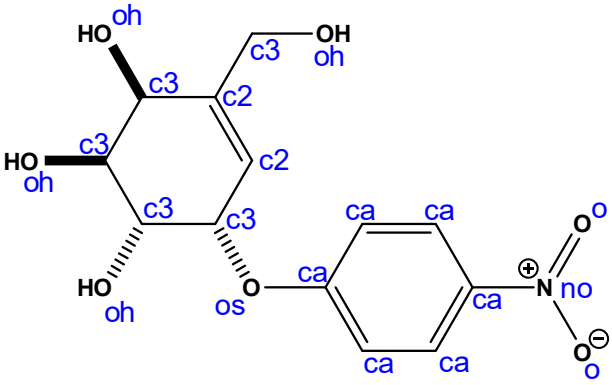
HC2	h1	0.1027	
HC3	h1	0.0937	
HC4	h1	0.0587	
H6a	h1	0.0337	
H6b	h1	0.0337	
H5a	ha	0.1560	
HO2	ho	0.4160	
HO3	ho	0.4220	
HO4	ho	0.4120	
HO6	ho	0.4100	
HR1	ha	0.1590	
HM1	ha	0.1725	
HM2	ha	0.1725	
HR2	ha	0.1590	

Table S10. Cartesian coordinates (in Å) of the QM atoms for the structure of the TS_{alk} substrate **3** optimized at DFT/MM level.

Atom	Coordinates		
C1	40.593	37.511	38.335
C2	41.995	37.795	37.871
C3	42.733	36.595	37.307
C4	42.549	35.418	38.275
C5	41.055	35.143	38.478
C6	40.767	34.184	39.605
CO1	38.771	38.176	36.096
CR1	38.542	39.498	36.593
CM1	37.545	40.309	36.11
CP	36.711	39.854	35.072
CM2	36.896	38.606	34.508
CR2	37.913	37.787	34.995
F2	41.941	38.824	36.931
NP	35.673	40.724	34.547
NR2	38.095	36.521	34.31
O1	39.665	37.399	36.597
O3	44.098	36.919	37.177
O4	43.198	35.717	39.472
O5	40.294	36.373	38.827
O6	39.39	33.837	39.588
OP1	35.571	41.85	35.022
OP2	34.951	40.304	33.653
OR1	39.022	35.799	34.645
OR2	37.322	36.218	33.404
H1	40.014	38.341	38.736
H2	42.492	38.177	38.775
H3	42.298	36.316	36.338
H4	42.961	34.521	37.791
H5	40.598	34.791	37.545
H6a	41.054	34.661	40.551
H6b	41.408	33.306	39.456
HR1	39.196	39.866	37.375
HM1	37.409	41.306	36.518
HM2	36.27	38.271	33.689
HO3	44.356	37.094	36.246
HO4	43.546	34.847	39.898
HO6	39.263	32.988	40.117

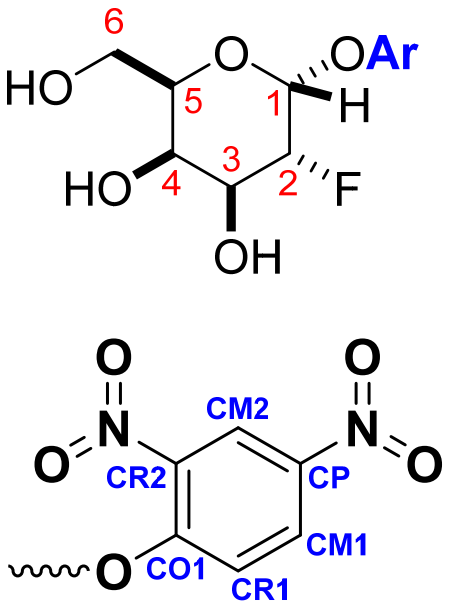

Table S11. Cartesian coordinates (in Å) of the QM atoms for the structure of the TS_{alk} of inhibitor **4** optimized at DFT/MM level.

Atom	Coordinates		
C1	43.918	56.533	41.369
C2	45.112	56.339	40.493
C3	46.274	57.237	40.915
C4	45.797	58.7	40.993
C5	44.49	58.828	41.767
C6	44.182	60.167	42.324
C5a	43.607	57.801	41.882
CO1	44.123	54.945	44.111
CR1	43.549	53.695	43.709
CM1	43.114	52.776	44.641
CP	43.228	53.057	46.015
CM2	43.712	54.307	46.444
CR2	44.113	55.236	45.516
O1	44.683	55.762	43.288
O2	45.523	54.979	40.454
O3	47.324	57.15	39.978
O4	45.571	59.174	39.688
O6	42.957	60.186	43.022
O1N	43.197	52.221	48.164
O2N	42.37	51.007	46.588
NO2	42.906	52.047	46.968
HC1	43.182	55.737	41.391
HC2	44.773	56.671	39.502
HC3	46.618	56.933	41.911
HC4	46.583	59.278	41.496
H6A	44.198	60.87	41.471
H6B	45.026	60.457	42.973
H5a	42.674	57.963	42.408
HO2	44.885	54.485	39.917
HO3	47.986	56.481	40.254
HO4	45.557	60.183	39.654
HO6	42.693	61.126	43.264
HR1	43.505	53.455	42.65
HM1	42.704	51.824	44.321
HM2	43.759	54.538	47.502
HR2	44.486	56.205	45.836

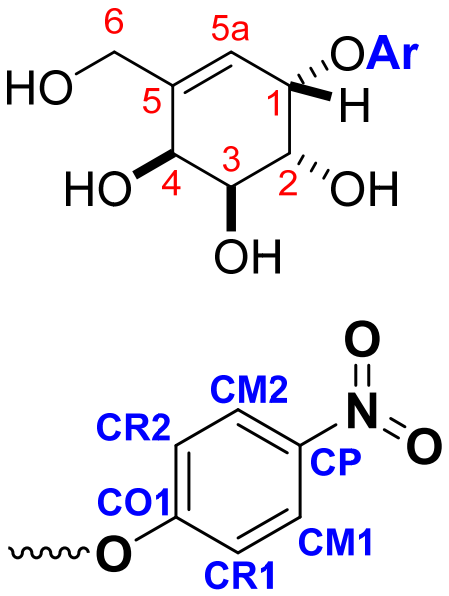

Figure S1: Least squares Michaelis-Menten fit of the kinetic data for the hydrolysis of the 4-nitrophenyl α-D-galactopyranoside **3** by WT *Tm*GalA. All experiments were performed at T = 37 °C, 50 mM buffer (MES buffer for pH 6.5, HEPES buffer for pH 7.0–7.5, glycylglycine buffer for pH 8.0–8.5, glycine-NaOH buffer for pH 9.0–10.0), and 0.1% BSA. The solid lines are the nonlinear least squares fit to a standard Michaelis-Menten equation.

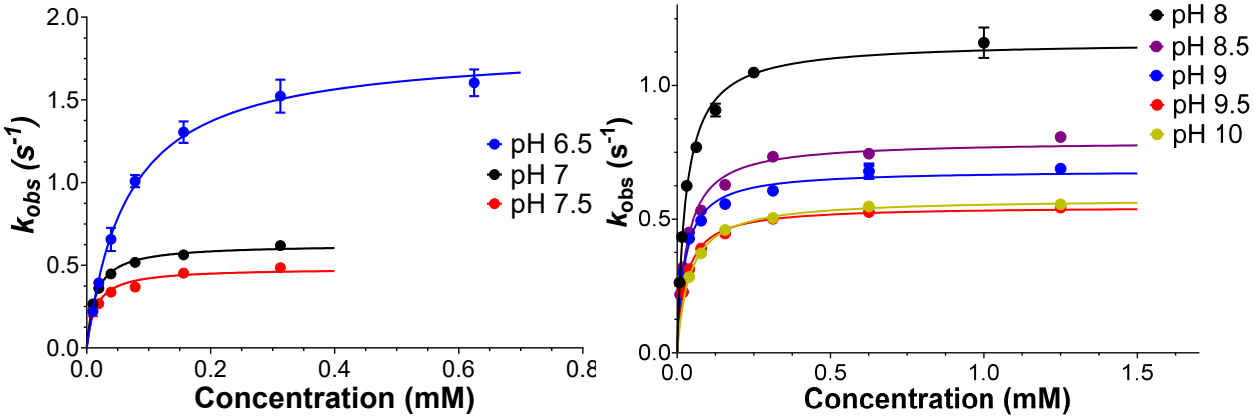

Figure S2: Least squares Michaelis-Menten fit of the kinetic data for the hydrolysis of the 4-methylumbelliferyl α-D-galactopyranoside **2** by WT *Tm*GalA. All experiments were performed at T = 37 °C, 50 mM buffer (MES buffer for pH 6.5, HEPES buffer for pH 7.0–7.5, glycylglycine buffer for pH 8.0–8.5, glycine-NaOH buffer for pH 9.0–10.0), and 0.1% BSA. The solid lines are the nonlinear least squares fit to a modified Michaelis-Menten equation that includes a substrate inhibition term.

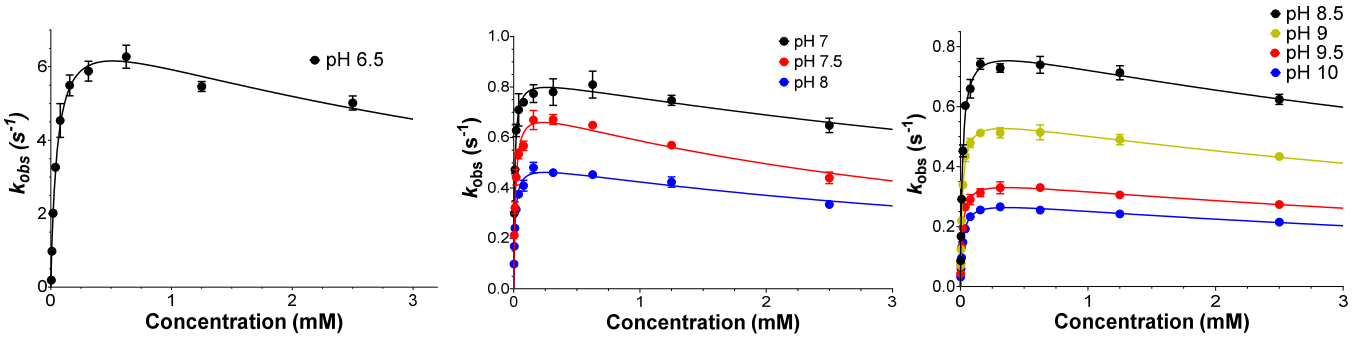

Figure S3: Least squares Michaelis-Menten fit of the kinetic data for the hydrolysis of the 6-fluoro-4-methylumbelliferyl β-D-melibioside **1** by WT TmGalA. All experiments were performed at T = 37 °C, 50 mM buffer (MES buffer for pH 6.5, HEPES buffer for pH 7.0–7.5, glycylglycine buffer for pH 8.0–8.5, glycine-NaOH buffer for pH 9.0–10.0), and 0.1% BSA. The solid lines are the nonlinear least squares fit to a modified Michaelis-Menten equation that includes a substrate inhibition term.

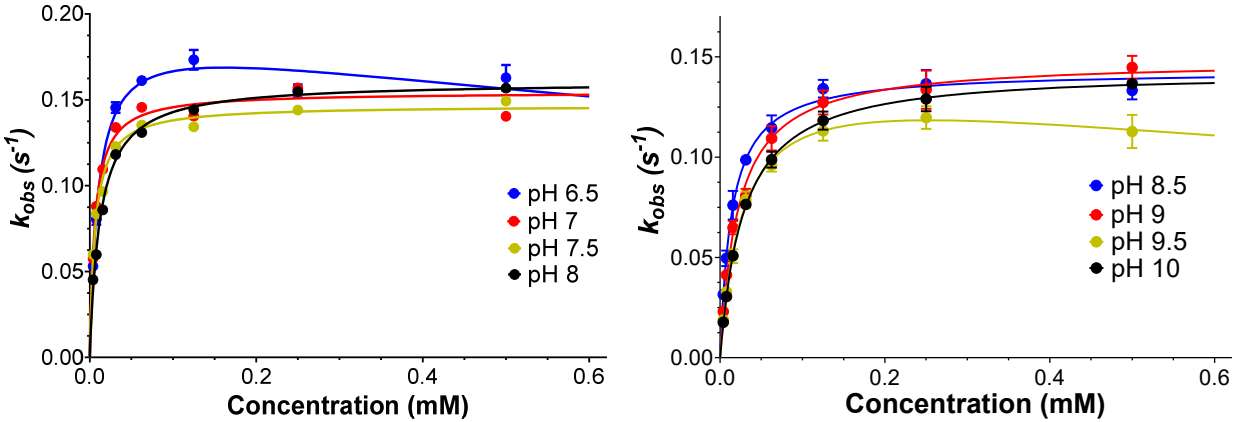

Figure S4: First-order loss of *Tm*GalA WT activity due to time-dependent inactivation by different concentrations of α-*galacto*-cyclophellitol **7** at different pH. All experiments were performed at T = 37 °C, 50 mM buffer (MES buffer for pH 6.5, glycylglycine buffer for pH 8.0–8.5, glycine-NaOH buffer for pH 10.0), and 0.1% BSA.

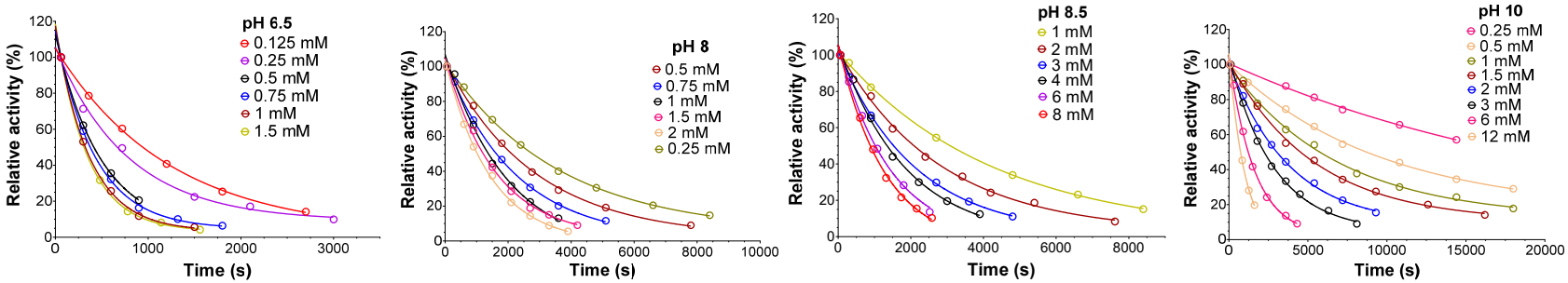

Figure S5: Michaelis Menten plot for the inactivation of *Tm*GalA WT α-*galacto*-cyclophellitol **7** at different pH. All experiments were performed at T = 37 °C, 50 mM buffer (MES buffer for pH 6.5, glycylglycine buffer for pH 8.0 and 8.5, glycine-NaOH buffer for pH 10.0, and 0.1% BSA. The solid lines are the nonlinear least squares fit to a standard Michaelis-Menten equation.

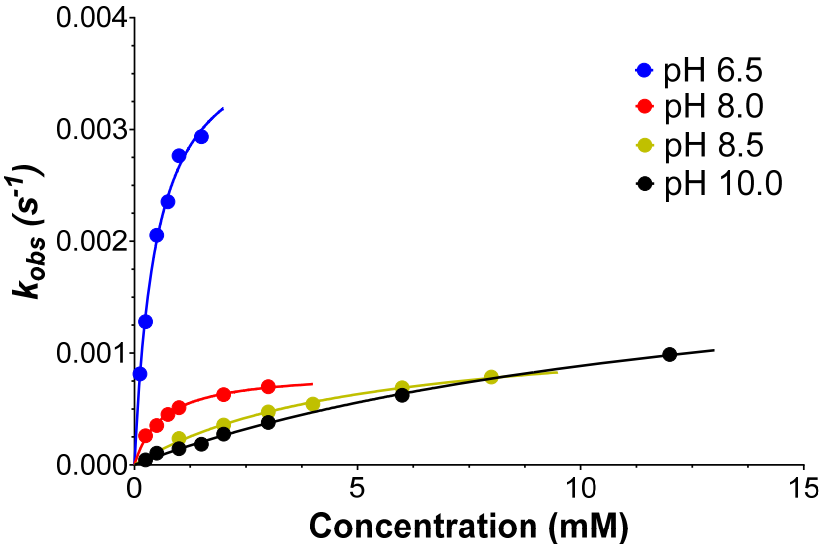

Figure S6: First-order loss of *Tm*GalA WT and variant enzyme activities due to time-dependent inactivation by different concentrations of α-*galacto*-cyclophellitol **7**. All experiments were carried out at T = 37 °C in 50 mM glycylglycine buffer, pH 8.0 and 0.1 % BSA.

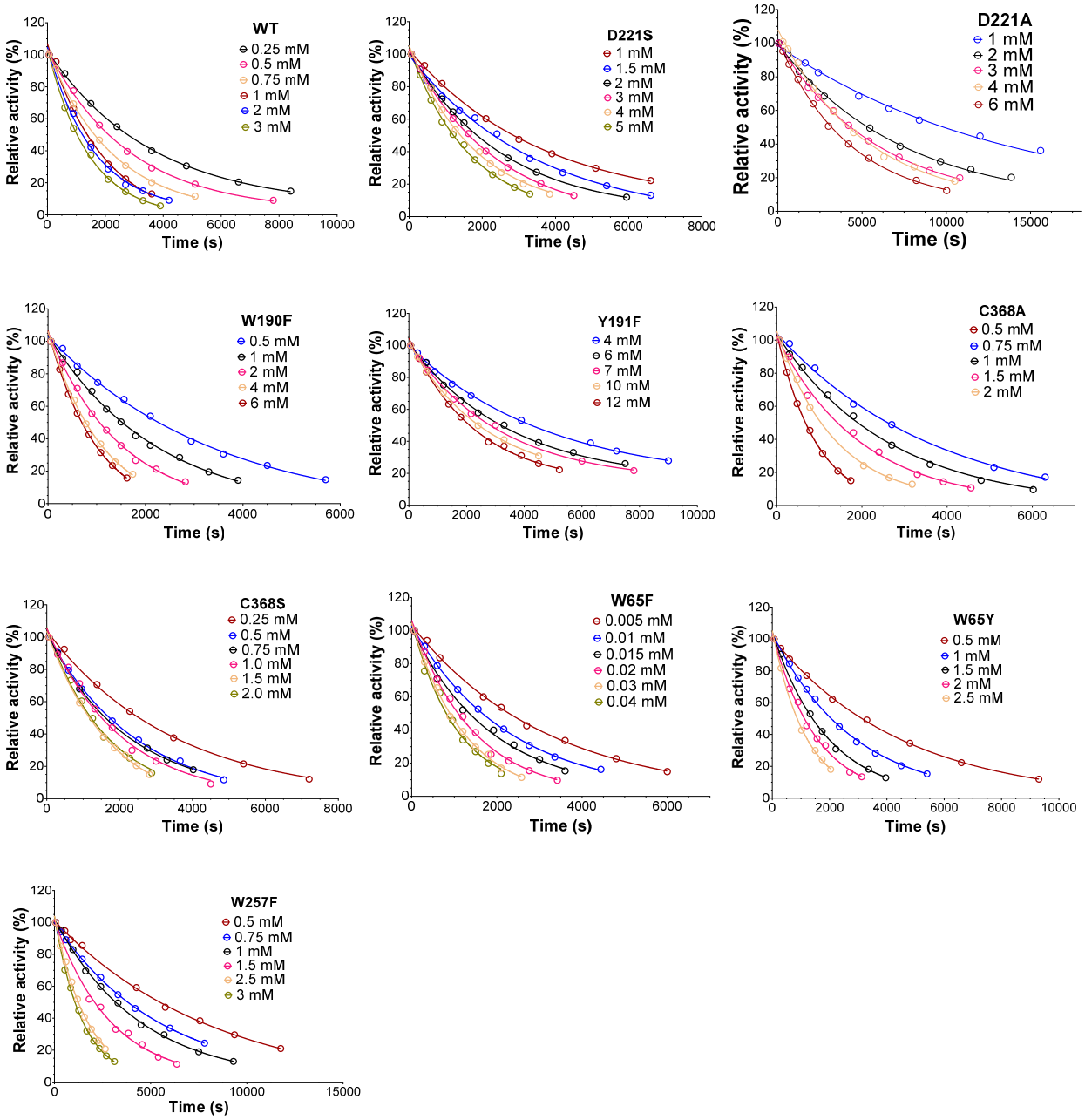

Figure S7: Michaelis Menten plot for the inactivation of *Tm*GalA WT and variants by α-*galacto*-cyclophellitol **7**. All experiments were carried out at T = 37 °C in 50 mM glycylglycine buffer, pH 8.0 and 0.1 % BSA. The solid lines are the nonlinear least squares fit to a standard Michaelis-Menten equation.

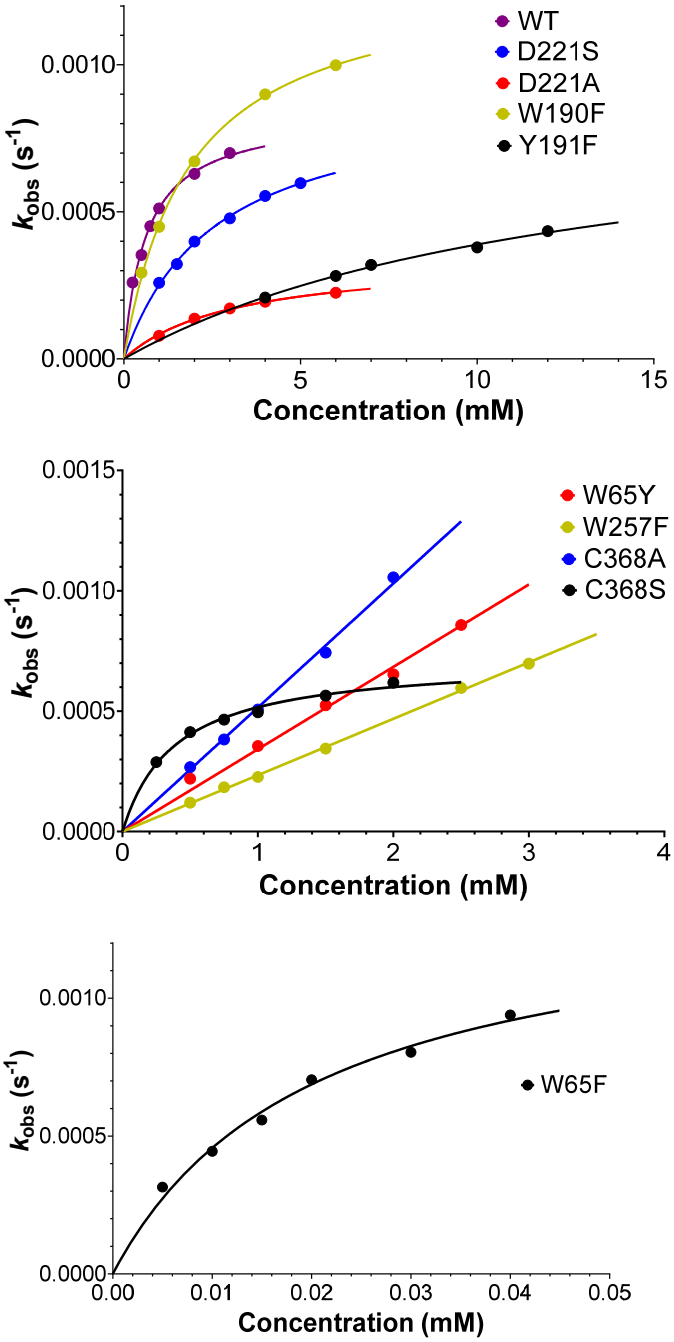

Figure S8: Least squares Michaelis-Menten fit of the kinetic data for the hydrolysis of the 6-fluoro-4-methylumbelliferyl β-D-melibioside **1**. All experiments were carried out at T = 37 °C in 50 mM glycylglycine buffer, pH 8.0 and 0.1% BSA.

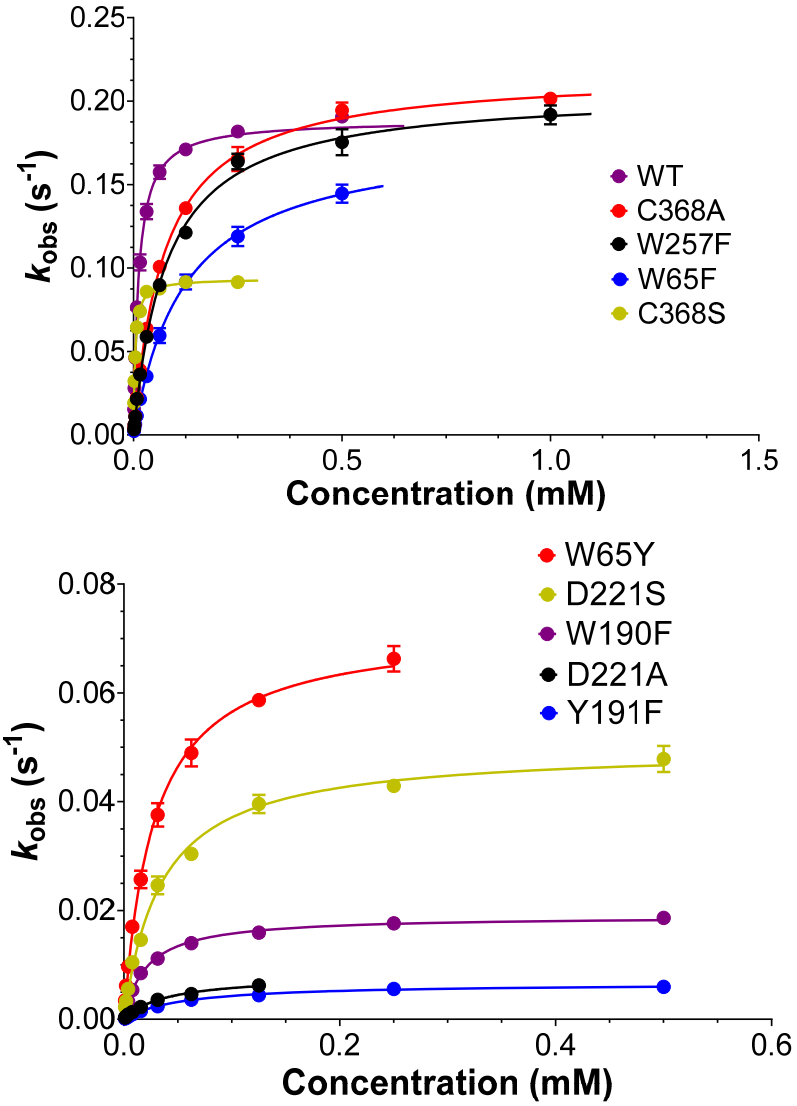

Figure S9: Least squares Michaelis-Menten fit of the kinetic data for the hydrolysis of the 4-nitrophenyl α-D-galactopyranoside **2**. All experiments were carried out at T = 37 °C in 50 mM glycylglycine buffer, pH 8.0 and 0.1% BSA.

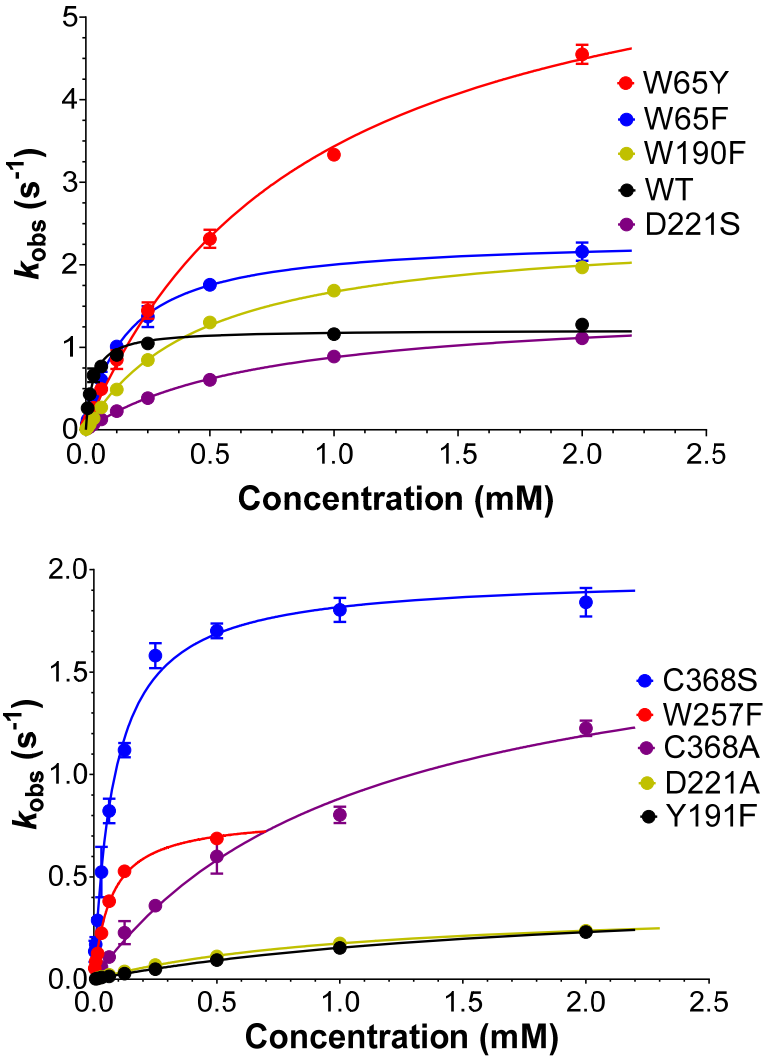

Figure S10: Least squares Michaelis-Menten fit of the kinetic data for the hydrolysis of the 2,4-dinitrophenyl 2-deoxy-2-fluoro-α-D-galactopyranoside **3**. All experiments were carried out at T = 37 °C in 50 mM glycylglycine buffer, pH 8.0 and 0.1% BSA.

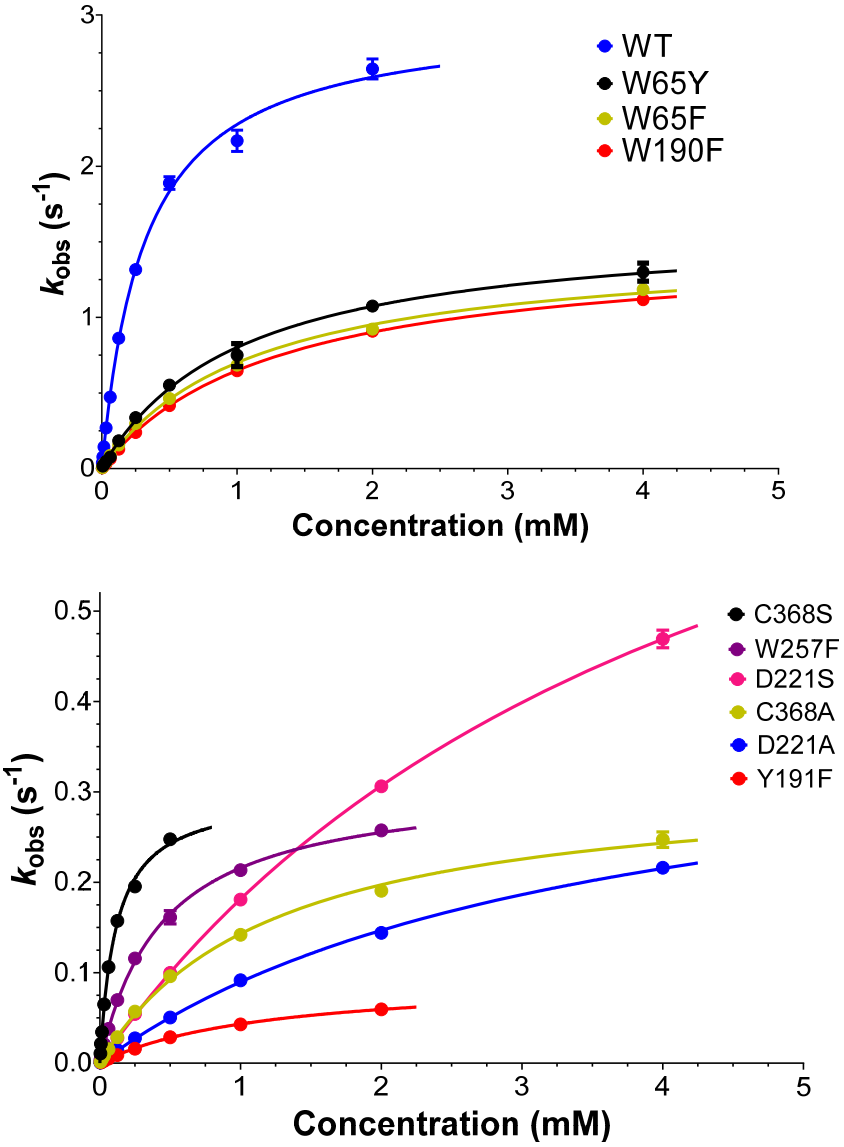

Figure S11: Least squares Michaelis-Menten fit of the kinetic data for the hydrolysis of the covalent inhibitor **4**. All experiments were carried out at T = 37 °C in 50 mM glycylglycine buffer, pH 8.0 and 0.1% BSA.

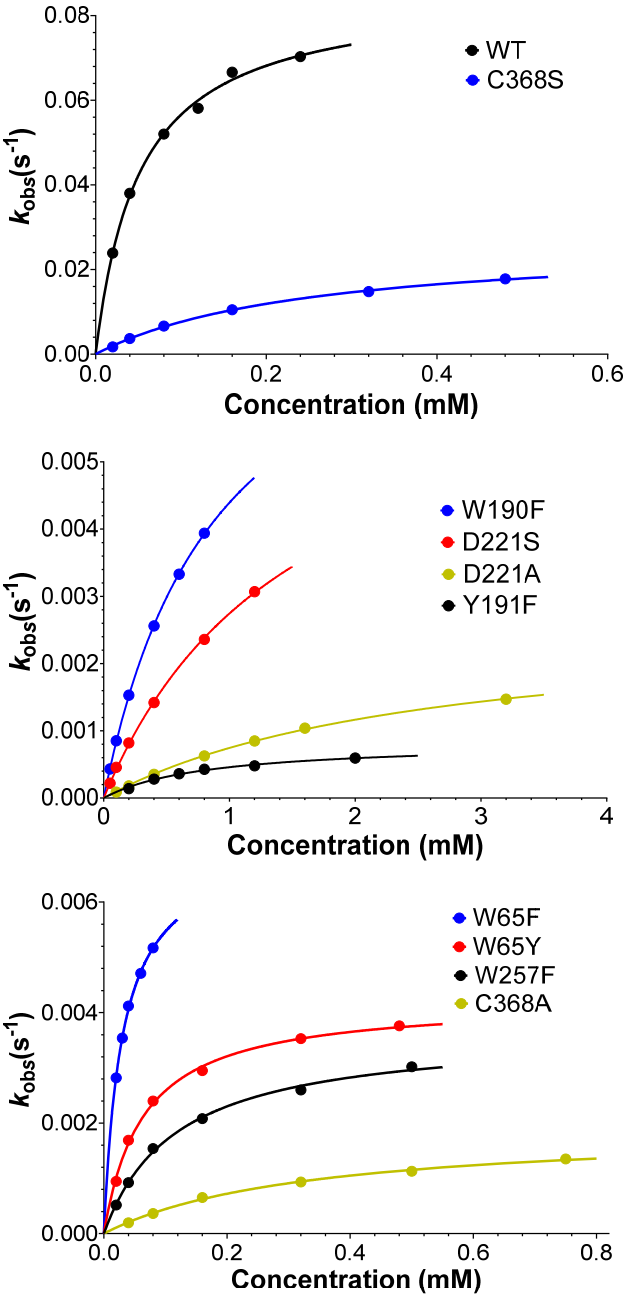

Figure S12: Least squares Michaelis-Menten fit of the kinetic data for the covalent inhibition by carbasugar **5**. All experiments were carried out at T = 37 °C in 50 mM glycylglycine buffer, pH 8.0 and 0.1% BSA.

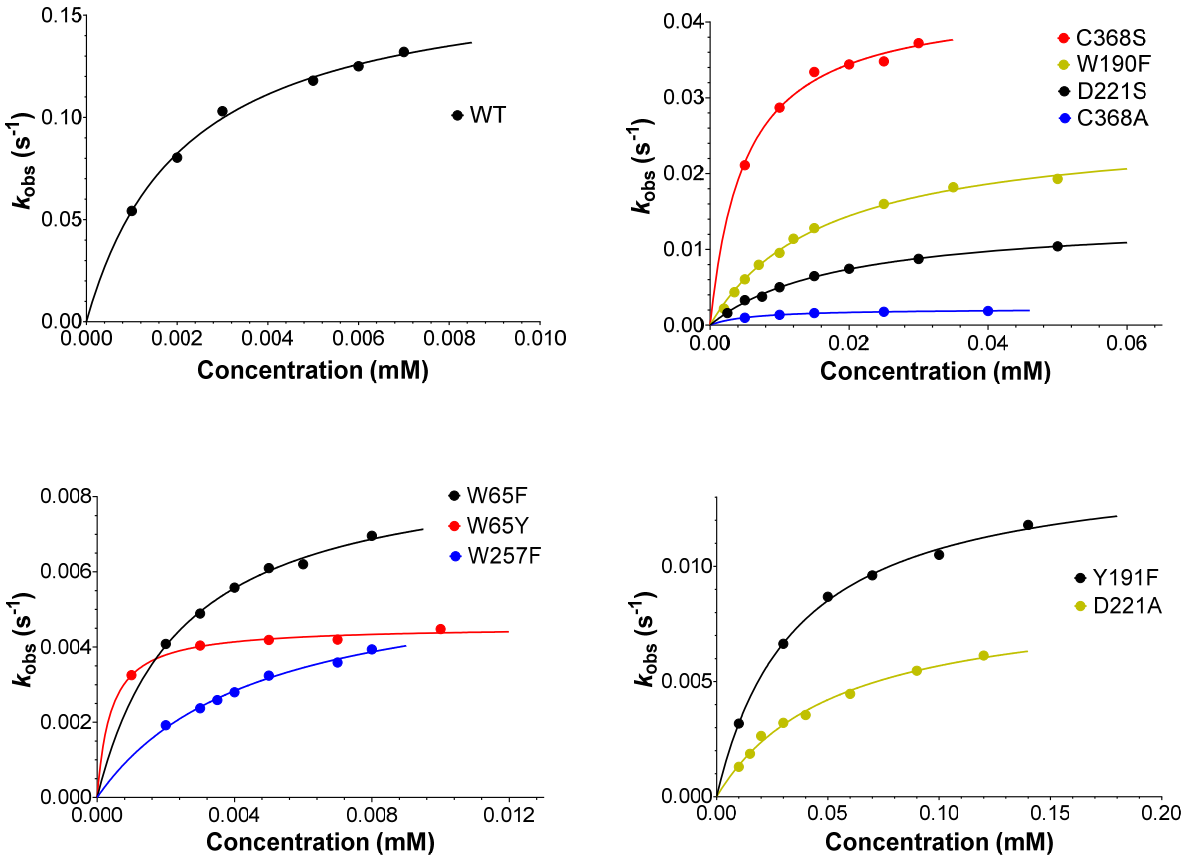

Figure S13: Least squares Michaelis-Menten fit of the kinetic data for the covalent inhibition by fluorocarbasugar **6**. All experiments were carried out at T = 37 °C in 50 mM glycylglycine buffer, pH 8.0 and 0.1% BSA.

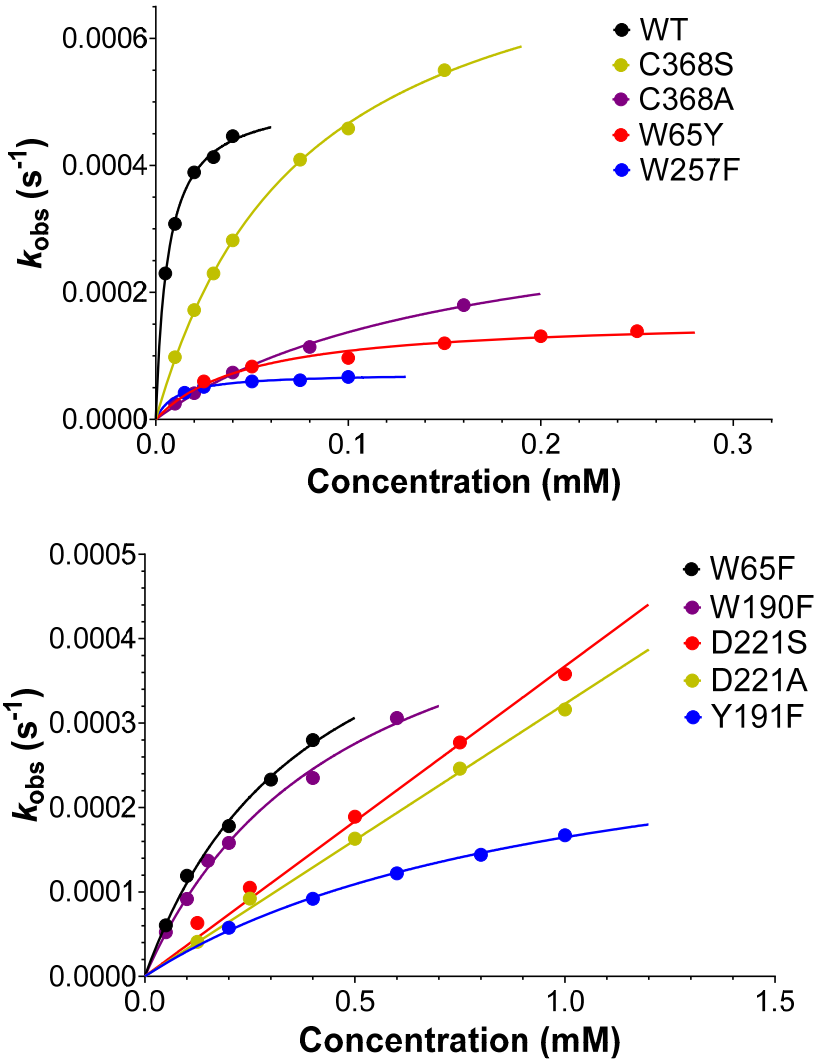

Figure S14: Co-crystal structure of wild-type *Tm*GalA in complex with the reaction product formed after turnover of carbasugar **4** (PDB 6GVD)[2] showing the extensive hydrogen-bonding network with the hydrolyzed covalent inhibitor bound in the active site. Note that residues lysine325, tyrosine191, and arginine383 have been truncated for clarity reasons.

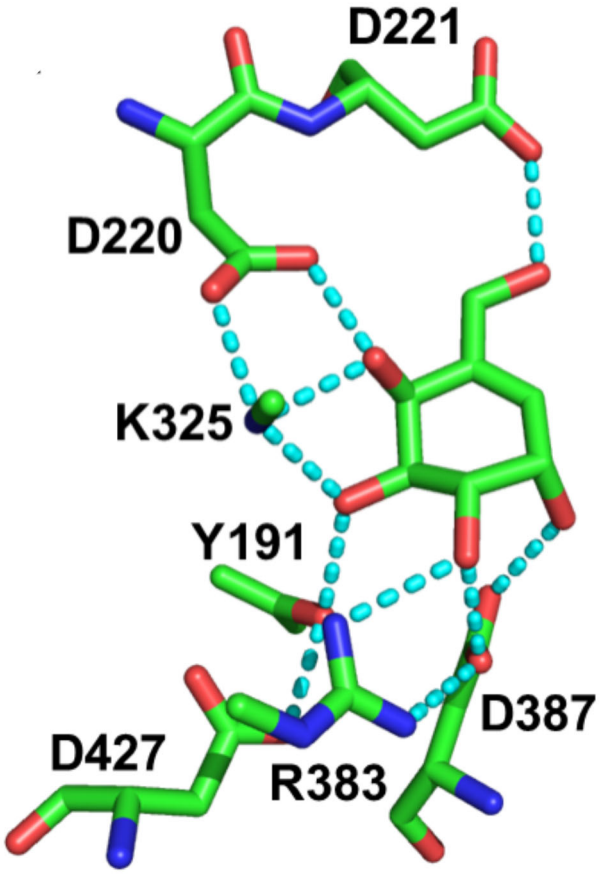

Figure S15: ^{1}H NMR spectrum of **1** in CD_3OD

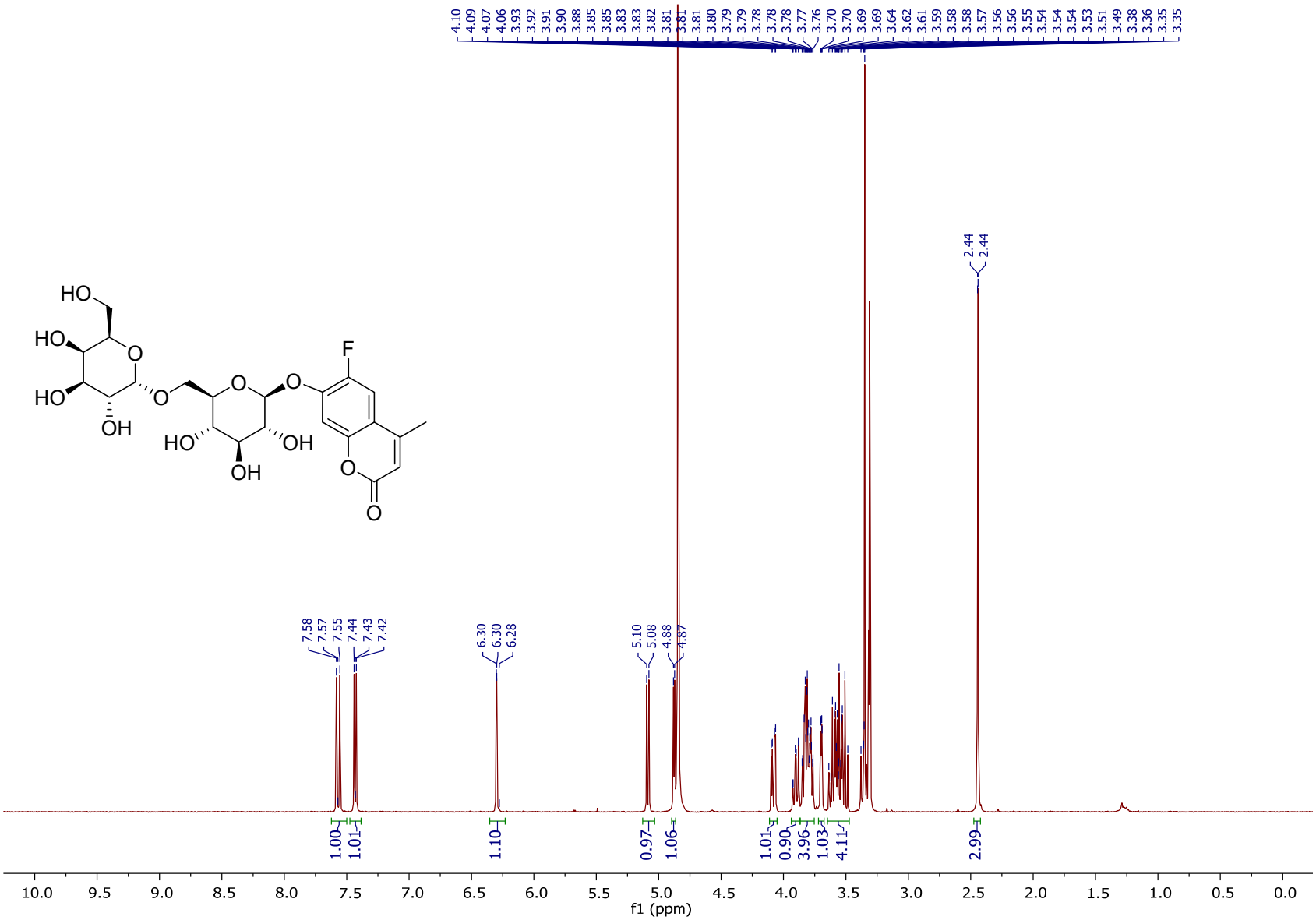

Figure S16: ^{13}C [^{1}H]NMR spectrum of **1** in CD_3OD

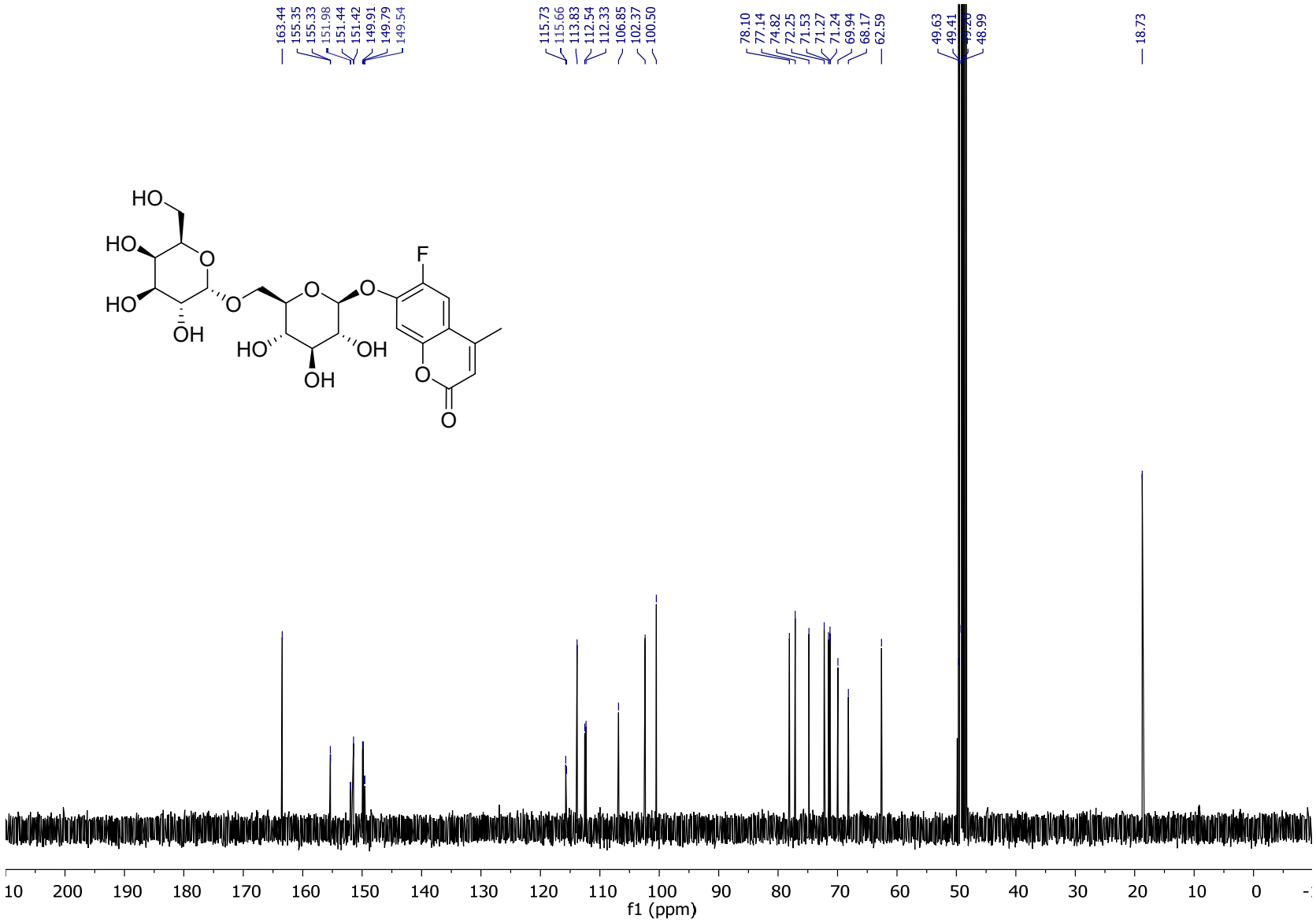

Figure S17: Time dependence of RMSD computed for the backbone atoms of the protein for substrate **3**. Total Energy during 10 ns MM MD simulations performed to equilibrate the starting structure generated from the X-ray structure.

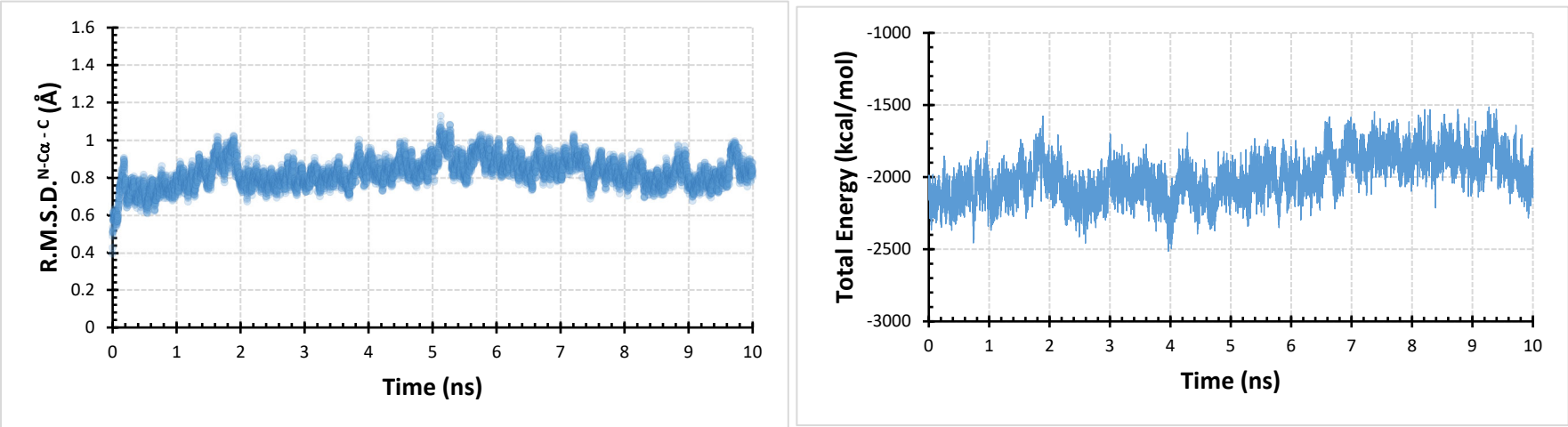

Figure S18: Time dependence of RMSD computed for the backbone atoms of the protein for inhibitor **4**. Total Energy during 10 ns MM MD simulations performed to equilibrate the starting structure generated from the X-ray structure.

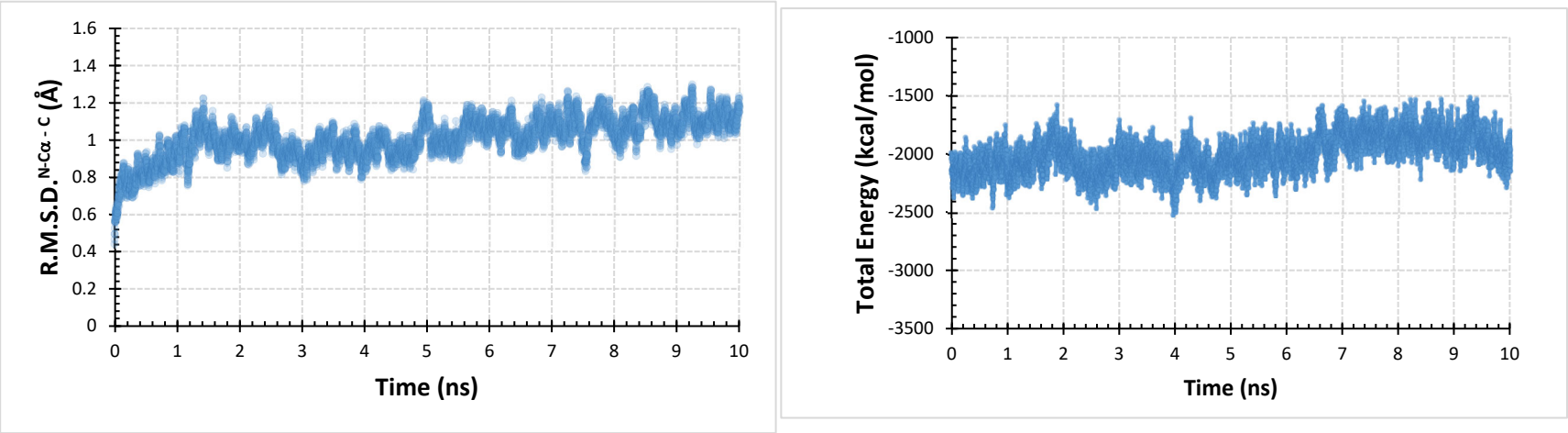

Figure S19: Schematic representation of the active site of *Tm*GalA. The grey region corresponds to atoms in the QM region in QM/MM calculations for the alkylation step of substrate **3** (left) and inhibitor **4** (right). Link atoms are indicated as black dots.

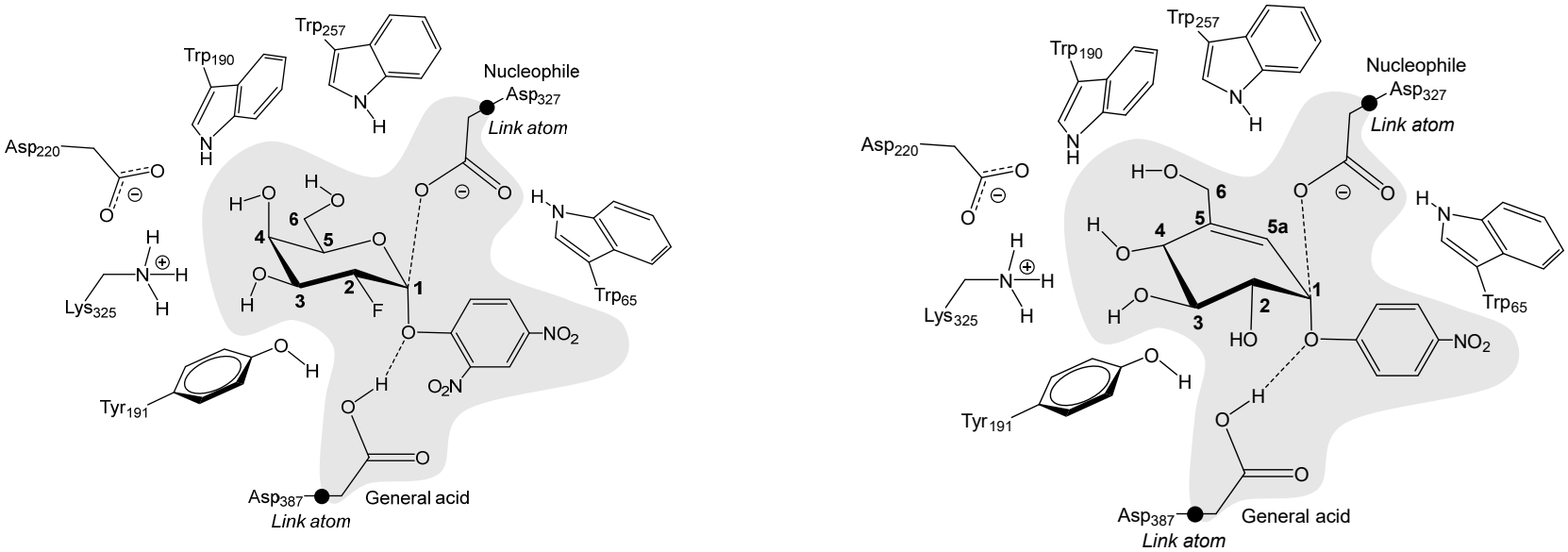

References

1. Ren, W.; Farren-Dai, M.; Sannikova, N.; Swiderek, K.; Wang, Y.; Akintola, O.; Britton, R.; Moliner, V.; Bennet, A. J., Glycoside hydrolase stabilization of transition state charge: New directions for inhibitor design. *Chem. Sci.* **2020**, *11*, 10488-10495.
2. Ren, W.; Pengelly, R.; Farren-Dai, M.; Shamsi Kazem Abadi, S.; Oehler, V.; Akintola, O.; Draper, J.; Meanwell, M.; Chakladar, S.; Świderek, K.; Moliner, V.; Britton, R.; Gloster, T. M.; Bennet, A. J., Revealing the mechanism for covalent inhibition of glycoside hydrolases by carbasugars at an atomic level. *Nat. Commun.* **2018**, *9*, 3243.